

The Mechanism for Ultrananocrystalline Diamond Growth: Experimental and Theoretical Studies

Paul William May¹ and Yuri A. Mankelevich²

¹School of Chemistry, University of Bristol, Cantock's Close, Bristol, BS8 1TS, United Kingdom

²Nuclear Physics Institute, Moscow State University, Moscow, 119992, Russian Federation

ABSTRACT

Ar/CH₄/H₂ gas mixtures have been used to deposit microcrystalline diamond, nanocrystalline diamond and ultrananocrystalline diamond films using hot filament chemical vapor deposition. A 3-dimensional computer model was used to calculate the gas phase composition for the experimental conditions at all positions within the reactor. Using the experimental and calculated data, we show that the observed film morphology, growth rate, and across-sample uniformity can be rationalized using a model based on competition between H atoms, CH₃ radicals and other C₁ radical species reacting with dangling bonds on the surface. Proposed formulae for growth rate and average crystal size are tested on both our own and published experimental data for Ar/CH₄/H₂ and conventional 1%CH₄/H₂ mixtures, respectively.

INTRODUCTION

Recently, so-called ultrananocrystalline diamond (UNCD) films have become a topic of great interest, since they offer the possibility of making smooth, hard coatings at relatively low deposition temperatures, which can be patterned to nm resolution.^{1,2} These differ from nanocrystalline diamond (NCD) films,³ since they have much smaller grain sizes (~2-5 nm), and have little or no graphitic impurities at the grain boundaries. Most reports of the deposition of these films describe using a microwave (MW) plasma CVD reactor and gas mixture of 1%CH₄ in Ar, usually with addition of 1-5% H₂.¹

We have previously reported the use of similar Ar/CH₄/H₂ gas mixtures to deposit microcrystalline diamond (MCD), NCD and UNCD in a hot filament (HF) reactor,⁴ with the compositional diagram for mixtures of Ar, CH₄ and H₂ being mapped out corresponding to the type of film grown. For the majority of the composition diagram, diamond films are deposited only in a very narrow region around [CH₄]/([CH₄]+[H₂]) ~ 0.5-6%, with UNCD films being deposited only in the region of the MCD/'no-growth' boundary.

Originally it was suggested⁵ that the C_2 radical played an important role in the growth mechanism for UNCD. However, recent work by ourselves^{6,7} and others⁸ has shown that C_2 is only a minority species close to the substrate surface and plays no significant role in growth. In our previous paper,⁷ we used a 2-dimensional model of the gas chemistry, including heat and mass transfer, in our HF reactors to understand the experimental observations. The conclusions led to a generalized mechanism⁷ for the growth of diamond by CVD which was consistent with all experimental observations, both from our group and from others in the literature.

The proposed mechanism involves competitive growth by all the C_1 radical species that are present in the gas mixture close to the growing diamond surface. Previous models only considered CH_3 since this is the dominant reactive hydrocarbon radical in standard H_2 -rich CVD gas mixtures. However, we found that in HFCVD reactors at high filament temperatures (*e.g.* $T_{fil} \sim 2700$ K), the concentration of the other C_1 radical species, in particular C atoms, near the growing diamond surface can become a significant fraction ($\sim 5\%$) of that of CH_3 , and so may contribute to the growth process.

In the model, abstraction of surface H atoms by gas phase atomic H are the reactions which drive the chemistry of growth. The various types of surface radical that result from abstraction are shown in Fig.1. We proposed that CH_3 remains the major growth species, and if this adds to a surface biradical site, $C_d^* - C_d^*$, (defined as two surface radical sites adjacent to one another, see Fig.1(d), the ‘dangling bonds’ on the surface are terminated and stabilized.¹⁵ For typical diamond CVD conditions, the fraction of available biradical sites is ~ 10 times lower than that of radical sites (Fig.1(b)), but CH_3 cannot add to the more abundant radical sites due to steric hindrance.⁹ Further hydrogen abstraction converts the surface CH_3 groups into bridging CH_2 groups, and repetition of this process allows the CH_2 groups to migrate across the surface until they meet a step-edge, at which point they will extend the diamond lattice leading to large regular crystals, and a MCD film, as usual.⁷ Thus, the prerequisites for MCD film formation are high H concentration (to generate sufficient surface biradical sites), high CH_3 concentration, and the rapid migration across the surface of CH_2 groups (catalysed by H atom abstractions).

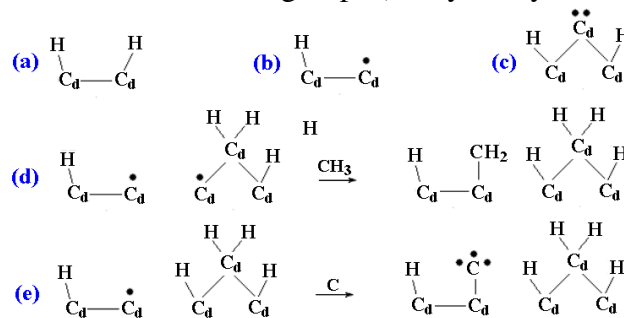


Figure 1. Schematic diagram of the various (100)-(2x1) dimer surface and bridge sites important for diamond growth and renucleation. (a) A hydrogen terminated diamond surface. (b) A surface radical site C_d^* . (c) A surface biradical site C_d^{**} . (d) A different type of surface biradical site, $C_d^* - C_d^*$, followed by its reaction with methyl to give a CH_2 surface group (ref.9). (e) The radical site also reacts with a C atom (or CH radical, not shown) to give a reactive surface adduct C_d^{**} .

However, as well as CH_3 addition, we assumed that C atoms or CH radicals (and also CH_2 but these have been neglected since their number density close to the substrate surface is much lower) could also be adsorbed on the surface. Due to their smaller size, atomic C and CH have less steric hindrance and can add to both surface biradical sites and radical sites (see Fig.1). Thus, even for low C atom concentrations $[C]/[CH_3] \sim 0.1$, their contribution to the growth rate

can become important since they can add to the more abundant radical sites. The resulting adduct structure C_d^{**} (see Fig.1(e)) would remain reactive since it would still contain dangling bonds, making this a very high energy site. The most likely fate for such reactive surface sites, considering that they are surrounded by a gas mixture containing a high concentration of H atoms and H_2 molecules, is that they are rapidly hydrogenated to CH_2 . If so, the subsequent reactions will be indistinguishable from attachment and growth by methyl. However, other possible fates for the reactive surface adducts are reaction with other gas-phase hydrocarbon radicals CH_x or restructuring of the surface. The role of such adducts as an initiator of renucleation processes requires additional theoretical study.

For the typical conditions used to deposit MCD/NCD and UNCD in a variety of different diamond CVD reactors (including MW and HF CVD reactors), the reactions of the surface adducts with atomic hydrogen which lead to continuous normal diamond growth are much more frequent events than the reactions with CH_x which ultimately could lead to renucleation. As long as the surface migration of CH_2 (induced by H abstractions) is much faster than adsorption of CH_3 , the aggregation of CH_2 bridge sites into continuous chains (void filling) will provide normal layer-by-layer {100} diamond growth.⁹ But as the ratio of gaseous CH_x/H increases, the initiation of next layer growth could proceed before all the voids in the current layer are filled. Thus, depending upon the gas mixture and reaction conditions used, the relative concentrations of each of these species close to the growing diamond surface (*e.g.* $[H]/[CH_3]$, $([C]+[CH])/[CH_3]$) determine the probability of a renucleation event occurring and average crystal sizes, $\langle d \rangle$, and hence the morphology of the subsequent film, be it MCD, NCD or UNCD.

In this paper we shall present further experimental and calculated data to support and refine the proposed mechanism outlined above. Due to space constraints, we shall restrict ourselves here to one set of deposition conditions (for UNCD). However, a far more detailed description of the model, along with comparisons of its predictions for MCD and NCD deposition conditions will be given elsewhere.¹⁰ We shall also present quantitative estimations of $\langle d \rangle$ and the growth rate, G , for UNCD growth.

EXPERIMENT

Films were deposited using a standard HF reactor operating at a pressure of 100 Torr using high purity Ar, CH_4 and H_2 as source gases. Mass flow controllers were used to control the ratios of the three gases. $[Ar]/([Ar]+[H_2])$ was kept constant at 80%, and that of $[CH_4]/([H_2]+[CH_4])$ at 1.5%, which puts it in the UNCD growth region of the Ar/ CH_4 / H_2 composition diagram.⁴ The filament was made from 0.25 mm-diameter Ta metal, wound around a 3 mm-diameter core to produce a 2 cm-long coil that was positioned 5.5 mm from the substrate surface. The filament temperature was kept constant at 2400°C and monitored using a 2-colour optical pyrometer. The substrate was single crystal Si (100) which had been manually abraded prior to deposition using 1-3 μm diamond grit, and then ultrasonically cleaned with propan-2-ol. The substrate sat on a separate heater to give additional uniform heating and to maintain it at a temperature of ~850-900°C (also measured using the optical pyrometer). Typical deposition times were 8 h.

MODELING

In our previous paper,⁷ we have carried out serial calculations for different methane fractions in H₂/Ar mixtures using a 2-dimensional model with coordinates of r (radial distance from the center of the substrate to the edge) and z (vertical distance from the substrate to the filament). We now keep the gas feed mixture constant, and use a 3-dimensional (3D) model, which is much more computationally time consuming, but more accurately describes the geometry of the hot region of coiled wire and the spatial profiles of species concentrations and growth rates. The 3D model has been specifically tailored to a reactor of this geometry.¹¹ The input parameters for the model were taken from the experimental values: pressure 100 Torr, filament temperature 2400°C, and Ar/H₂/CH₄ gas flows, as appropriate. The model comprises three blocks, which describe (i) activation of the reactive mixture (*i.e.* gas heating and catalytic H atom production at the filament surface), (ii) gas-phase processes (heat and mass transfer and chemical kinetics), and (iii) gas-surface processes at the substrate.

The 3D shape of the experimental filament (a coiled wire) was approximated in rectangular (x,y,z) coordinates as six parallel filaments (in the y direction) bounding the equivalent cylindrical hot volume $-1.5 < x < 1.5$ mm, $-10 < y < 10$ mm, $5.5 < z < 8.5$ mm, where the z axis is perpendicular to the substrate surface and the filament axis, and axis x is parallel to the substrate surface and perpendicular to the filament axis. The point (0,0,0) corresponds to the substrate center.

The gas-phase chemistry and thermochemical input is taken from the GRI-Mech 3.0 detailed reaction mechanism for C/H/Ar gas mixtures.¹² As in previous studies^{4,13,14,15} the conservation equations for mass, momentum, energy, and species concentrations, together with appropriate initial and boundary conditions, thermal and caloric equations of state, are each integrated numerically until steady-state gas temperature and radicals distributions are attained. This process yields spatial distributions of the gas temperature, T_{gas} , the flow field, and the various species number densities and mole fractions. The incorporation of gas-surface reactions, involving H abstraction to form surface sites, and the subsequent reactions of these sites with H and hydrocarbon radicals, serve to alter the gas composition close to the surface. The main effect of these reactions is to reduce the H atom concentrations directly above the growing diamond surface, which in turn affects the hydrocarbon radical concentration and has major implications for subsequent growth.

RESULTS

The variation of film morphology and properties with varying gas composition have been presented previously,⁷ so in this paper we shall restrict our discussion to the spatial uniformity for one set of growth conditions. The films grown in our HF reactor under the growth conditions mentioned above, satisfied a number of criteria consistent with being UNCD. First, the films showed no evidence of facets, even at very high magnification.¹⁰ Second, we observed the presence of the 1150-1190 cm⁻¹ Raman line which has been attributed¹⁶ to sp^2 carbon in *trans*-polyacetylene-like molecules trapped at the nanograin boundaries. This peak is often considered as being a signature for UNCD, despite its origin being sp^2 carbon. Third, transmission electron microscopy (TEM) analysis revealed the films to be composed of randomly-oriented crystals with grains <10 nm in size, with lattice spacings consistent with that of diamond. The growth

rate of the UNCD films was low, around $0.1 \mu\text{m h}^{-1}$ in the center of the substrate directly beneath the HF (0,0,0) and non-uniform, with a marked drop-off in growth rate with distance from the substrate center (see Fig.3).

Modelling of the gas phase chemistry allows gas temperature and gas phase concentrations to be calculated as a function of (x,y,z) coordinates. The distance between the bottom of the hot filament and the substrate was $z \sim 5.5 \text{ mm}$, consistent with that in the experiments. In the model for the HFCVD reactor there are two reactor-specific parameters, which are not well-determined. These are (i) the temperature discontinuity ΔT (the difference between filament temperature T_f and the gas temperature near the filament, T_{nf}) and (ii) the catalytic H_2 dissociation rate Q on the filament surface (*i.e.* the net production of H atoms per second per unit area). For these, as before⁷ we used values of ΔT and Q similar to those adopted in previous HFCVD reactor studies in standard 1% CH_4/H_2 mixtures at gas pressures of 20 Torr.^{14,15}

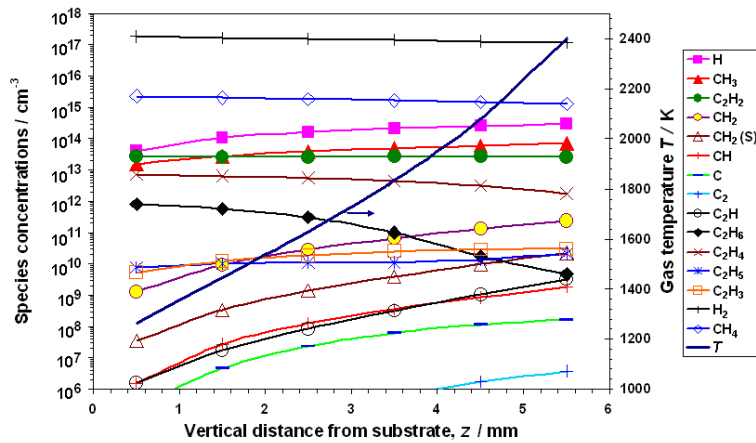
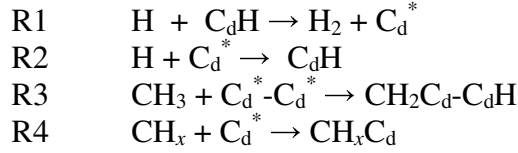


Figure 2. Concentrations of various gas phase species as a function of z , the vertical distance between the substrate centre ($z = 0$) and the filament ($z = 5.5 \text{ mm}$), as well as the variation of the gas temperature, T . The calculation was performed using values of Q and ΔT so as to fit the experimental growth rates.

The calculated gas phase species distribution between the filament and substrate ($0 < z < 5.5 \text{ mm}$, $x = 0$) is shown in Fig.2. This shows that the concentration of atomic H near the surface decreases as a result of gas-surface reactions. Since reactions with atomic H generate hydrocarbon radicals, this drop in $[\text{H}]$ has the effect of decreasing the concentrations of *all* the other gas phase radicals near the surface. However, the depletion of CH_x concentration specifically by gas-surface chemical reactions is negligible on this scale. In other words, the surface is an important sink only for H atoms, and does not provide a significant loss mechanism for any of the hydrocarbon species.

As in standard MCD growth conditions, we see in Fig.2 for our HF UNCD growth conditions that near to the growing surface there is a relatively high concentration of CH_3 but much lower concentrations of all the other C_1 and C_2 radicals. With CH_3 being the dominant reactive hydrocarbon radical, diamond growth will occur via three basic reactions R1-R3 (see below). Reaction R1 is the abstraction of a terminating hydrogen by a gas phase H atom, producing a reactive surface radical site. The reverse of this reaction, together with R2, lead to the addition of an H atom to the surface radical site, thereby returning the diamond surface to its normal hydrogen-terminated state with a base CH_2 surface group. Reaction R3 is the methyl addition step which propagates the diamond structure and maintains the symmetry of the lattice.

For deposition conditions which have high concentrations of other C₁ species (CH_x, x<3) near the growth surface (*e.g.* during UNCD growth), there is another set of reactions R4 possible, for each value of *x*:



Depending upon which C₁ species adds to the substrate, there are different rate laws (with correspondingly different rate constants¹⁰) which govern the kinetics, and hence the growth rate. It is possible to estimate the contribution to the growth rate, *G* (in μm h⁻¹), of the important C₁ species, using formulae stated in Ref. 17:

$$G_{\text{CH}_3} = 3.8 \times 10^{-14} T_{\text{ns}}^{0.5} [\text{CH}_3] R^2 \quad (1)$$

$$G_{\text{CH}_x} = 3.9 \times 10^{-14} T_{\text{ns}}^{0.5} [\text{CH}_x] R \quad (2)$$

where *T_{ns}* is the gas temperature near the substrate (obtained from the modelling results) and CH_x is for *x* = 0,1,2. *R* is the fraction of surface radical sites given by $R = \text{C}_d^* / (\text{C}_d^* + \text{C}_d\text{H})$, where C_d^{*} and C_dH are the respective densities of open- and hydrogen-terminated surface sites. (The probability of the surface site becoming a biradical site is, therefore, *R*²). This fraction, *R*, mainly depends on the rate constants for the surface H abstraction and addition reactions, and can be calculated using the data and following the procedure outlined in our previous paper.⁶ For example, neglecting the effects of CH_x upon radical site density *R*, so that

$$R = 1 / \{ 1 + k_2/k_1 + k_{-1}[\text{H}_2]/(k_1[\text{H}]) \} \quad (3)$$

and using the known dependences of the coefficients *k_i* (see ref. 10) we obtain

$$R = 1 / \{ 1 + 0.3 \exp(3430 / T_s) + 0.1 \exp(-4420 / T_s) [\text{H}_2]/[\text{H}] \} \quad (4)$$

Here *T_s* is the substrate temperature in Kelvin, with [H] and [H₂], respectively, being the atomic and molecular hydrogen concentrations near the substrate.

Given the concentrations of species near the surface shown in Fig.2, two mechanisms which affect the normal diamond structure propagation can be highlighted:

- a) The appearance of a surface C atom with *two* dangling bonds C_d^{**}, followed by adsorption of other gas-phase hydrocarbon radicals or restructuring of the surface. The possibility of such renucleation mechanisms requires additional study.
- b) The growth of the next layer before filling all the voids of the current layer, which can occur at high CH₃ addition rate,⁹ or more exactly, at elevated gaseous Σ[CH_x]/[H] ratios, *x*<4.

It can be shown¹⁰ that the limit of the normal growth length (*i.e.* the crystal size) will be approximated by

$$\langle d \rangle = 2k_1 [\text{H}] (1 - R) l / (k_3 [\Sigma\text{CH}_x] R^2) \quad (5)$$

Using Eq.(5) with Eqs.(1)-(4), average crystal sizes and growth rates can be calculated and compared with experimental data. Figure 3 shows the calculated growth rates and crystal sizes, for our deposition conditions, along with the experimental values. The growth rate can be seen to drop off as x increases, *i.e.* the film gets thinner towards the edge of the substrate, and this closely mirrors the experimental trend. Experimentally, the crystal size in the center of the substrate (where the process was optimized) is $<d>$ $<i.e.>$ UNCD). However, $<d>$ rapidly increases towards the edge of the sample, giving grain sizes $\sim 0.45 \mu\text{m}$ at the edge. These observations are consistent with the observations of other workers that MCD and UNCD can be deposited simultaneously in different places on the same substrate.¹⁸ This trend reflects the localized heat source arising from a hot filament, and would be much less pronounced in a microwave system. The modeling mirrors this trend in $<d>$, however, the absolute magnitude of $<d>$ near the center of the substrate is overestimated by a factor of ~ 10 .

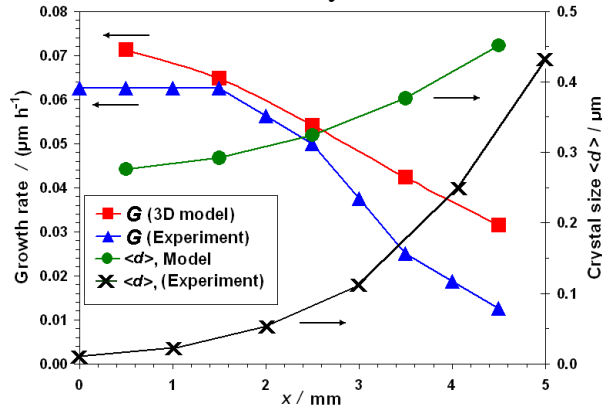


Figure 3. Total growth rate and average crystal size calculated as a function of distance x from the center of the substrate.

CONCLUSIONS

In this paper we have presented further evidence to support and refine our model^{6,7} for the growth mechanisms of the various forms of diamond film produced in a HF reactor using both Ar/H₂/CH₄ and traditional CH₄/H₂ gas mixtures. We have shown that the observed film morphology, growth rate, crystal size, and the variation of these with distance from the filament can be rationalized using a model based on competition to react with dangling bonds on the surface by H atoms, CH₃ radicals and other C₁ species.

The modelling described in this paper has some inaccuracies due to the need to fit the growth rates to a parameter for the filament efficiency, Q . In the MCD regime, the model works quite well, and predicts growth rates and crystal sizes reasonably accurately (see Ref.10 for details). However, when the nucleation rate approaches that required for UNCD growth, the model becomes less accurate – although it still predicts grain sizes to within an order of magnitude, as well as the trends in growth rate and grain size with distance from the filament. Nevertheless, using this model, we have shown that a knowledge of the gas phase concentrations near the growing diamond surface can be used to estimate the growth rate and average crystal size during diamond HFCVD, and thereby to predict whether the film morphology will be MCD, NCD or UNCD, along with its across-sample uniformity.

ACKNOWLEDGMENTS

The authors would like to thank Edward Crichton and other members of the Bristol diamond group and S. Schwarz for useful discussions. YuAM wishes to thank RF Leading Scientific Schools program (Project SS-7101.2006.2) and ISTC grant 2968/2005.

REFERENCES

- ¹ D. M. Gruen, O. A. Shenderova, A. Ya. Vul' (Eds.), *Synthesis, Properties and Applications of Ultrananocrystalline Diamond*, Springer, 2005 (NATO Science Series part II, vol. 192).
- ² X. Xiao, J. Birrell, J. E. Gerbi, O. Auciello and J. A. Carlisle, *J. Appl. Phys.*, **96**, 2232 (2004).
- ³ O. A. Williams, M. Daenen, J. D'Haen, K. Haenen, J. Maes, V. V. Moshchalkov, M. Nesládek, D. M. Gruen, *Diamond Relat. Mater.*, **15**, 654 (2006).
- ⁴ P. W. May, J. A. Smith, Yu. A. Mankelevich, *Diamond Relat. Mater.*, **15**, 345 (2006).
- ⁵ D. Zhou, T. G. McCauley, L. C. Qin, A. R. Krauss and D. M. Gruen, *J. Appl. Phys.*, **83**, 540 (1998).
- ⁶ P. W. May, J. N. Harvey, J. A. Smith, Yu. A. Mankelevich, *J. Appl. Phys.*, (2006), **99**, 104907.
- ⁷ P. W. May, Yu. A. Mankelevich, *J. Appl. Phys.*, (2006), **100** (2006) 024301.
- ⁸ J. R. Rabeau, P. John, J. I. B. Wilson and Y. Fan, *J. Appl. Phys.*, **96**, 6724 (2004).
- ⁹ S. Skokov, B. Weiner, M. Frenklach, *J. Phys. Chem.*, **98**, 7073 (1994).
- ¹⁰ P. W. May, Yu. A. Mankelevich, *J. Appl. Phys.* (2007) in press.
- ¹¹ Y. A. Mankelevich, A. T. Rakhimov and N. V. Suetin, *Diamond Relat. Mater.*, **7**, 1133 (1998).
- ¹² G. P. Smith, D. M. Golden, M. Frenklach, N. W. Moriarty, B. Eiteneer, M. Goldenberg, C. T. Bowman, R. K. Hanson, S. Song, W. C. Gardiner, Jr., V. V. Lissianski, and Z. Qin, <http://www.me.berkeley.edu/gri-mech/>
- ¹³ Y. A. Mankelevich, N. V. Suetin, M. N. R. Ashfold, J. A. Smith and E. Cameron, *Diamond Relat. Mater.*, **10**, 364 (2001).
- ¹⁴ M. N. R. Ashfold, P. W. May, J. R. Petherbridge, K. N. Rosser, J. A. Smith, Y. A. Mankelevich and N. V. Suetin, *Phys. Chem. Chem. Phys.*, **3**, 3471 (2001).
- ¹⁵ J. A. Smith, J. B. Wills, H. S. Moores, A. J. Orr-Ewing, Yu. A. Mankelevich and N. V. Suetin, *J. Appl. Phys.*, **92**, 672 (2002).
- ¹⁶ A. C. Ferrari and J. Robertson, *Phys. Rev. B*, **63**, 121405 (2001).
- ¹⁷ Y. A. Mankelevich, N. V. Suetin, M. N. R. Ashfold, W. E. Boxford, A. J. Orr-Ewing, J. A. Smith and J. B. Wills, *Diamond Relat. Mater.*, **12**, 383 (2003).
- ¹⁸ Y. K. Liu, Y. Tzeng, C. Liu, P. Tso, I. N. Lin, *Diamond Relat. Mater.*, **13**, 1859 (2004).